

Identification and Characterization of the Dermal Panniculus Carnosus Muscle Stem Cells

Neia Naldaiz-Gastesi,^{1,2,3} María Goicoechea,^{2,3} Sonia Alonso-Martín,⁴ Ana Aiastui,^{2,3} Macarena López-Mayorga,⁵ Paula García-Belda,^{3,6} Jaione Lacalle,^{1,2,7} Carlos San José,⁸ Marcos J. Araúzo-Bravo,^{9,10} Lidwine Trouilh,^{11,12,13} Véronique Anton-Leberre,^{11,12,13} Diego Herrero,¹⁴ Ander Matheu,^{10,15} Antonio Bernad,¹⁴ José Manuel García-Verdugo,^{3,6} Jaime J. Carvajal,⁵ Frédéric Relaix,⁴ Adolfo Lopez de Munain,^{2,3,16,17} Patricia García-Parra,^{1,2,3,*} and Ander Izeta^{1,18,*}

¹Tissue Engineering Laboratory, Bioengineering Area

²Neuroscience Area

Instituto Biodonostia, San Sebastián 20014, Spain

³CIBERNED, Instituto de Salud Carlos III, Madrid 28029, Spain

⁴INSERM U955-E10, Université Paris Est, Faculté de Médecine, IMRB U955-E10, Creteil 94000, France

⁵Molecular Embryology Team, Centro Andaluz de Biología del Desarrollo, Sevilla 41013, Spain

⁶Laboratorio de Neurobiología Comparada, Instituto Cavanilles, Universidad de Valencia, Valencia 46980, Spain

⁷Faculty of Medicine and Nursing, UPV-EHU, San Sebastián 20014, Spain

⁸Animal Facility and Experimental Surgery

⁹Computational Biology and Systems Biomedicine

Instituto Biodonostia, San Sebastián 20014, Spain

¹⁰KERBASQUE, Basque Foundation for Science, Bilbao 48013, Spain

¹¹INSA, UPS, INP, LISBP, Université de Toulouse, 31077 Toulouse, France

¹²INRA, UMR792, Ingénierie des Systèmes Biologiques et des Procédés, 31400 Toulouse, France

¹³CNRS, UMR5504, 31400 Toulouse, France

¹⁴Immunology and Oncology Department, Spanish National Center for Biotechnology (CNB-CSIC), Madrid 28049, Spain

¹⁵Cellular Oncology Group, Oncology Area, Instituto Biodonostia, San Sebastián 20014, Spain

¹⁶Faculty of Medicine and Nursing, Department of Neurosciences, UPV-EHU, San Sebastián 20014, Spain

¹⁷Department of Neurology, Hospital Universitario Donostia, San Sebastián 20014, Spain

¹⁸Department of Biomedical Engineering, School of Engineering, Tecnun-University of Navarra, San Sebastián 20009, Spain

*Correspondence: pgarcia@nanogune.eu (P.G.-P.), ander.izeta@biodonostia.org (A.I.)

<http://dx.doi.org/10.1016/j.stemcr.2016.08.002>

SUMMARY

The dermal *Panniculus carnosus* (PC) muscle is important for wound contraction in lower mammals and represents an interesting model of muscle regeneration due to its high cell turnover. The resident satellite cells (the bona fide muscle stem cells) remain poorly characterized. Here we analyzed PC satellite cells with regard to developmental origin and purported function. Lineage tracing shows that they originate in *Myf5*⁺, *Pax3/Pax7*⁺ cell populations. Skin and muscle wounding increased PC myofiber turnover, with the satellite cell progeny being involved in muscle regeneration but with no detectable contribution to the wound-bed myofibroblasts. Since hematopoietic stem cells fuse to PC myofibers in the absence of injury, we also studied the contribution of bone marrow-derived cells to the PC satellite cell compartment, demonstrating that cells of donor origin are capable of repopulating the PC muscle stem cell niche after irradiation and bone marrow transplantation but may not fully acquire the relevant myogenic commitment.

INTRODUCTION

The dermal *Panniculus carnosus* (PC) muscle sits below the dermal fat layer and on top of the subcutaneous adipose tissue and fascia (Wojciechowicz et al., 2013). It is a fast-twitch muscle of vestigial nature in humans (Novakov et al., 2008), but otherwise ubiquitous in mammals. The PC has generally smaller fibers than other muscles with increased size heterogeneity and higher than usual regenerative myofibers (Brazelton et al., 2003). Being mainly composed of type II fibers, the PC muscle is thought to provide rodent loose skin with twitching and thermoregulation capacities (Greenwood, 2010), as well as promoting contraction (Watts et al., 1958) and supporting revascularization (Hughes and Dann, 1941) of full-thickness excisional wounds. Besides a long-sought clarification of its

functional role, a better understanding of PC in animal models and humans would be instrumental for plastic surgery and subcutaneous drug delivery studies alike (McDonald et al., 2010). However, this unique muscle remains ill characterized. From the stem cell biology viewpoint, specific data on non-limb muscle satellite cells (the bona fide muscle stem cells) are scarce (Randolph and Pavlath, 2015). PC satellite cell biology may be particularly interesting as a model system due to the accessibility, dispensability for survival, and increased regeneration rate of this muscle. In addition, the PC is distinctively positioned to understand the physiological role (if any) of hematopoietic stem cell (HSC) fusion to myofibers and their differentiation after transplantation (Ferrari et al., 1998), a little studied phenomenon that may be related to exposure of fused HSC-derived nuclei to *MyoD*-expressing



myofibers (Dellavalle et al., 2011). In the absence of injury, the rate of bone marrow-derived cell incorporation to PC is highly significant when compared with the physiologically irrelevant rates achieved by other muscle groups (Brazelton et al., 2003; Corbel et al., 2003; Sherwood et al., 2004b). The reasons underlying the increased incorporation of non-resident cells to PC remain unclear but may be related to increased cellular turnover in the PC.

The exact developmental origin of PC satellite cells has yet to be determined. Throughout development of the trunk and limb muscles, there is continuity between fetal muscle “founder” cells and adult satellite cells, as the latter appear to derive from the central dermomyotome of the somite (Gros et al., 2005; Kassar-Duchossoy et al., 2005; Relaix et al., 2005; Schienda et al., 2006). Specifically, at the embryonic day 10.5 (E10.5) central dermomyotome in mice, $En1^+$ cells generate muscle together with interscapular brown fat bundles and dermis (Atit et al., 2006). These data were confirmed by follow-up of $Pax7^{CE-\beta Gal^+}$ cells traced at E9.5 that labeled the PC (Lepper and Fan, 2011). However, the specific contribution of these early embryonic precursors to the adult PC satellite cell pool remains unknown. In this work, we have analyzed the PC muscle stem cells with regard to developmental origin and purported function, as well as the contribution of bone marrow-derived cells to the PC satellite cell pool after bone marrow transplantation.

RESULTS

Dorsal PC Satellite Cells Belong to the $Myf5^+$ Cell Lineage and Express $Pax3/Pax7$ during Development

The PC muscle sits below dermal adipose tissue in the mouse and is composed of striated fibers, as shown by the expression of $Mrf4$ (alkaline phosphatase [AP])⁺ (Kassar-Duchossoy et al., 2004) and sarcomeric myosin heavy chain (MyHC) (Figures 1A and 1B). The dorsal PC is known to arise from dermomyotomal precursors, but no lineage tracing study has yet addressed the origin of the canonical satellite cells in this muscle. Since a majority of adult muscle satellite cells derive from $Myf5^+$ progenitors (Biresi et al., 2013; Gayraud-Morel et al., 2012; Kuang et al., 2007) and express $Pax3/Pax7$ at later stages, the use of $Myf5$, $Pax3$, and $Pax7$ cell lineage-tracing models may help to dissect the cellular contribution at successive developmental stages (Figure 1C). To determine the developmental origin of PC, we crossed Cre recombinase-expressing transgenic lines with $R26YFP$ and $ROSA^{mTmG}$ reporter mouse strains and pursued in situ localization of reporter-expressing cells by performing immunofluorescence analyses in dorsal skin sections. As expected, PC fibers expressed the fluorescent reporters when cells were

marked by the $Myf5^{Cre^{Sor}}$, $Pax3^{Cre/+}$, and $Pax7^{CreERT2/+}$ lineage-tracing constructs (Figures 1D–1F). By transmission electron microscopy (TEM), we confirmed that PC satellite cells were located below the basal lamina and presented electron-dense nuclei with highly condensed chromatin patches and relatively small and undifferentiated cytoplasm (Figure 1G, asterisk). In situ, PC satellite cells of adult skin express MYF5 but no detectable PAX3, as determined by the expression of surrogate marker nLacZ (nuclear localized LacZ; Figures 1H and 1I). As canonical satellite cells, PC satellite cells are $PAX7^+$ (Figure 1J, higher-magnification image shown in inset 1J') and derive from the $Myf5^+$ lineage (Figure 1K). However, we were concerned with the reportedly widespread expression of $R26YFP$ when crossed with the $Myf5^{tm3(cre)Sor}$ mouse model (Eppig et al., 2015 and data not shown). To clarify tracing of $Myf5^+$ cell lineage, we generated and crossed a Cre-expressing mouse ($B195AP-Cre$) that marked a more restricted subset of $Myf5^+$ cells (Figure S1; more data on this strain are presented below). The more restricted $Myf5$ lineage-tracing strain confirmed detection of $EYFP^+$ cells in a satellite cell position, located between the plasmalemma and the basement membrane of the PC myofibers (Figure 1L). In summary, the lineage-tracing studies shown here confirm that, similar to other trunk muscles, PC satellite cells originate in $Myf5^+$, $Pax3/Pax7^+$ cell populations.

Muscle Cell Turnover Increases in Response to Injury to the PC with No Detectable Contribution of PC Satellite-Derived Cells to the Wound Bed

PC muscle is thought to be particularly regenerative, as determined by fiber morphology and the higher incorporation of bone marrow-derived cells compared with other muscles by cell-fusion events (Brazelton et al., 2003). To help us understand the determinants of PC turnover in homeostasis and response to wounding, we crossed $Pax7^{CreERT2/+}$ mice with the $ROSA^{mTmG}$ reporter line to trace the $Pax7$ -derived lineage by EGFP expression over the short term after tamoxifen (TMX) induction (Figure 2A). Full-thickness skin-punch wounds (that included the epidermis, dermis, dermal fat, and PC layers; Figure 2B) were performed and histological sections of the wounded area analyzed at days 5 and 10 post injury (Figures 2C and 2D). In the negative control (absence of TMX), no EGFP⁺ fiber was detected in the PC (Figures 2E and 2H). After TMX injection but in the absence of injury, $Pax7$ lineage tracing was induced and significant expression of the reporter gene under the control of $Pax7$ was found within fibers, most likely as a result of the incorporation of $Pax7$ -derived (EGFP⁺) cells to PC myofibers (Figures 2F, 2I, 2K, and 2L). In response to wounding, EGFP⁺ myofibers further increased (Figures 2G, 2J, and 2M) indicating that, while the PC seems to be markedly regenerative even under homeostatic

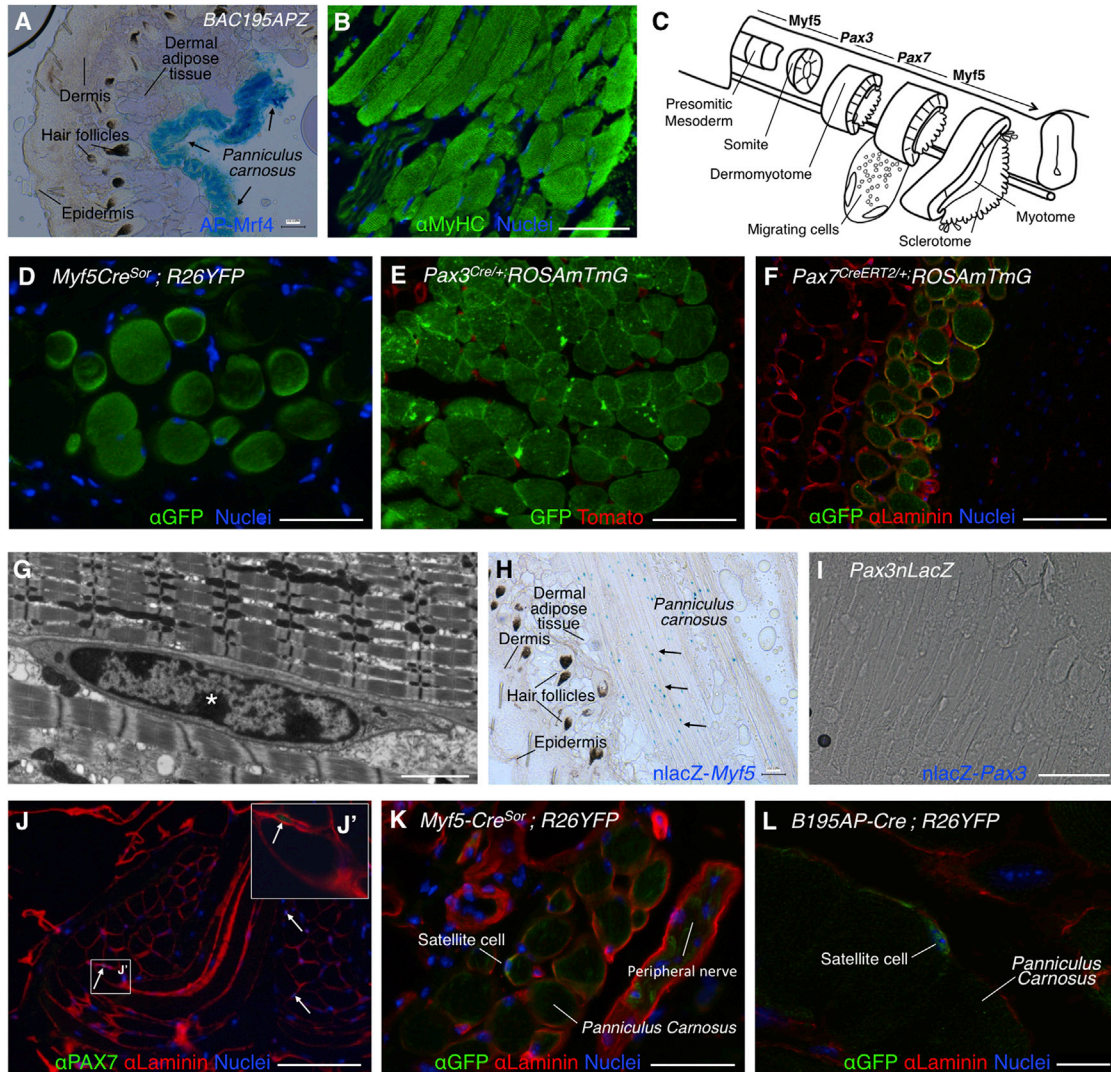


Figure 1. Elucidation of the Developmental Origin of PC Muscle and Satellite Cells

(A and B) Structure and localization of the PC. Histological sections of dorsal skin showing the presence of AP-*Mrf4*⁺ fibers (in *B195APZ* mice) (A) and striated MyHC⁺ fibers (in wild-type mice) (B).

(C) Schematic representation of embryonic muscle development from presomitic mesoderm to myotome formation (modified from Buckingham and Rigby, 2014). Sequential expression of *Myf5* (at the PSM), *Pax3*, *Pax7*, and again *Myf5* (at the somite) transcription factors is depicted at the top.

(D) *Myf5*⁺ lineage traced by immunofluorescence with anti-GFP antibody of *Myf5Cre^{SOR};R26YFP* dorsal skin sections.

(E) *Pax3*⁺ lineage traced by fluorescence of GFP and Tomato in *Pax3^{Cre/+}* dorsal skin sections.

(F) *Pax7*⁺ lineage traced by immunofluorescence with anti-GFP and anti-Laminin antibodies of *Pax7^{CE}* dorsal skin sections.

(G) TEM image of PC satellite cell ultrastructure from ultrathin skin sections. Asterisk indicates condensed chromatin patch.

(H) Histological section of dorsal skin showing the localization of *nlacZ-Myf5*⁺ cells (arrows) (in *B195APZ* mice).

(I) In *Pax3nLacZ* mice, no staining of the PC was observed indicating that PC satellites are *nlacZ-Pax3*-negative cells.

(J) Immunofluorescence with anti-PAX7 antibody demonstrates *Pax7*⁺ cells (arrows) in a satellite cell position underlying Laminin⁺ basement membrane. (J') Higher-magnification inset.

(K) Satellite cell marked by anti-GFP antibody in *Myf5Cre^{SOR};R26YFP* mice.

(L) Satellite cell marked by anti-GFP antibody in *B195AP-Cre;R26YFP* mice. Nuclei were counterstained with Hoechst 33258 (blue).

Scale bars represent 100 μm in all panels with the exception of (G) (2 mm) and (L) (10 μm). See also Figure S1.

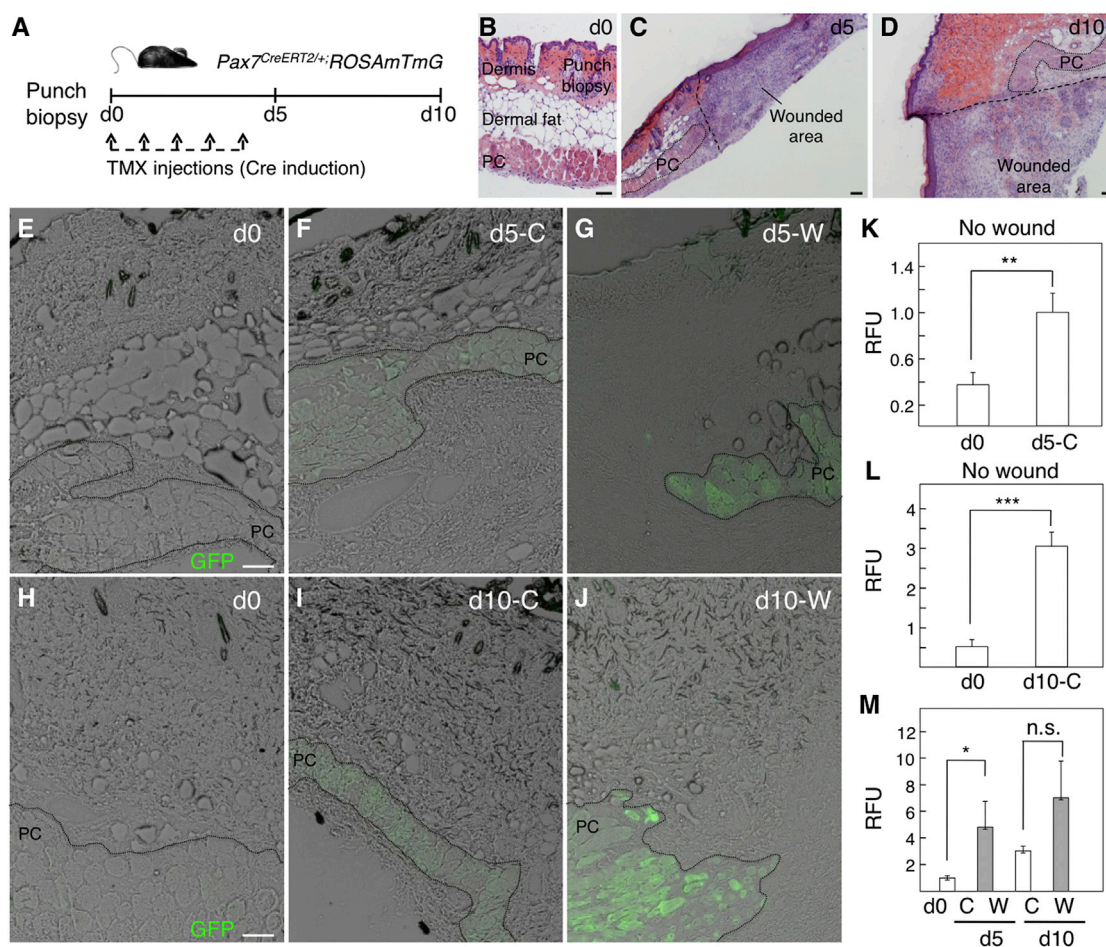


Figure 2. Characterization of the PC Regenerative Capacity in Homeostasis and in Short-Term Response to Wounding

(A) Outline of experimental design.

(B–D) Dorsal skin sections stained with H&E show the punch biopsy at day (d) 0 (B), and the wounded area at day 5 (C) and day 10 (D) post injury.

(E–J) GFP fluorescence in histological sections showing a control (C) area at day 0 (E and H), day 5 (F), and day 10 (I), and showing a wounded (W) area at day 5 (G) and day 10 (J).

(K–M) Quantification of the relative fluorescence units (RFU) present in the PC area. Comparisons between RFU of day 0 and day 5 in a control area (K), between day 0 and day 10 in a control area (L), and between control areas at days 0, 5, and 10 and wounded areas at days 5 and 10 (M) are shown. Bars represent means \pm SD in which the RFU were calculated in ImageJ from one to seven independent sections (N = 3 mice; n = 1 experiment). * $p < 0.05$, ** $p < 0.01$, *** $p < 0.001$; n.s., not significant.

Scale bars, 100 μ m.

conditions, the insult induced a further increase in cell turnover within the PC and the formation of new fibers.

A putative role of activated PC satellite cell progeny in wound contraction has been suggested (Munz et al., 1999), although to our knowledge direct contribution of PC-derived cells to the newly formed granulation tissue has not been experimentally observed. To test whether the PC satellite cell progeny contributes to the wound bed, we induced *Pax7^{CreERT2/+}; ROSAmTmG* mice with TMX 1 month in advance to ensure that all PC satellites were traced by *EGFP* expression (Figure 3A), and full-thick-

ness punch biopsies were performed as before (Figures 3B–3D). In this long-term assay, no contribution of PC satellite cell-derived (*EGFP⁺*) cell was evident in the wound bed up to day 10 post injury (Figures 3E–3L). Since regenerative fibers may be distinguished by the expression of embryonic forms of myosin (Schiaffino et al., 2015), staining with anti-MyHC3 antibody (DiMario et al., 1991) confirmed the existence of numerous regenerative myofibers in the PC (Figure S2). These results indicated that PC satellite cells are committed to muscle regeneration upon skin and muscle wounding, and that their progeny does not contribute

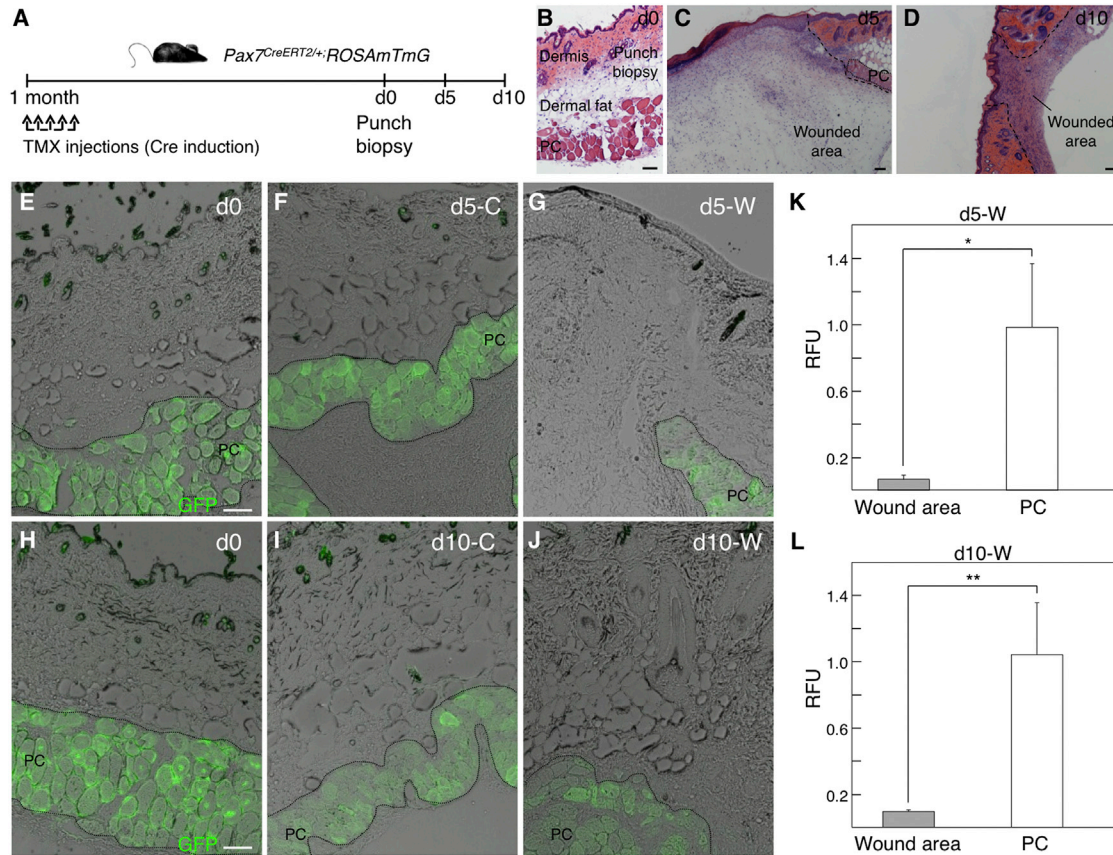


Figure 3. No Detectable In Vivo Contribution of PC-Derived Satellite Cells to the Dermal Compartment in Homeostasis or in Long-Term Response to Wounding

(A) Outline of experimental design. d, day; TMX, tamoxifen.

(B–D) Dorsal skin sections stained with H&E show the punch biopsy at day 0 (B), and the wounded area at day 5 (C) and day 10 (D) post injury.

(E–J) GFP fluorescence in histological sections showing a control (C) area at day 0 (E and H), day 5 (F), and day 10 (I), and showing a wounded (W) area at day 5 (G) and day 10 (J).

(K and L) Quantification of the relative fluorescence units (RFU) present in the PC and wound areas. Comparisons between RFU at PC and wound (W) areas at days 5 (K) and 10 (L) are shown. Bars represent means \pm SD in which the RFU were calculated in ImageJ from two to seven independent sections (N = 3 mice; n = 1 experiment). * $p < 0.05$, ** $p < 0.01$.

Scale bars, 100 μ m. See also [Figure S2](#).

to the wound bed and thus presents no obvious role in promoting full-thickness wound contraction.

Contribution of Bone Marrow-Derived Cells to the PC Satellite Cell Compartment

An intriguing possibility unresolved by previous studies was that bone marrow-derived cells, which engraft in significant numbers into PC muscle in the absence of injury ([Brazelton et al., 2003](#)), could contribute to the adult PC satellite cell pool. BMI1 is a transcription factor that is expressed in most adult stem cells, including satellite cells of skeletal muscle ([Robson et al., 2011](#)). To analyze whether bone marrow-derived cells contributed to the PC

satellite cell pool, we used recipient *Bmi1-Cre;YFP* mice (i.e., animals expressing YFP in satellite cells) that had been irradiated and successfully transplanted with donor RFP⁺ bone marrow cells from *Act-RFP* mice ([Figure 4A](#); [Valiente-Alandi et al., 2015](#)). As expected, animals transplanted with bone marrow showed a sizable contribution of RFP⁺ cells to the PC myofibers (6.95% positive fibers), which was within the expected range ([Figures 4B and 4C](#); [Brazelton et al., 2003](#)). Importantly, the contribution of donor cells to the satellite cell compartment had not been previously analyzed. We detected cells of donor origin in a satellite position (RFP⁺; [Figure 4D](#)) in the PC muscle of transplant recipients. To shed light on their functional

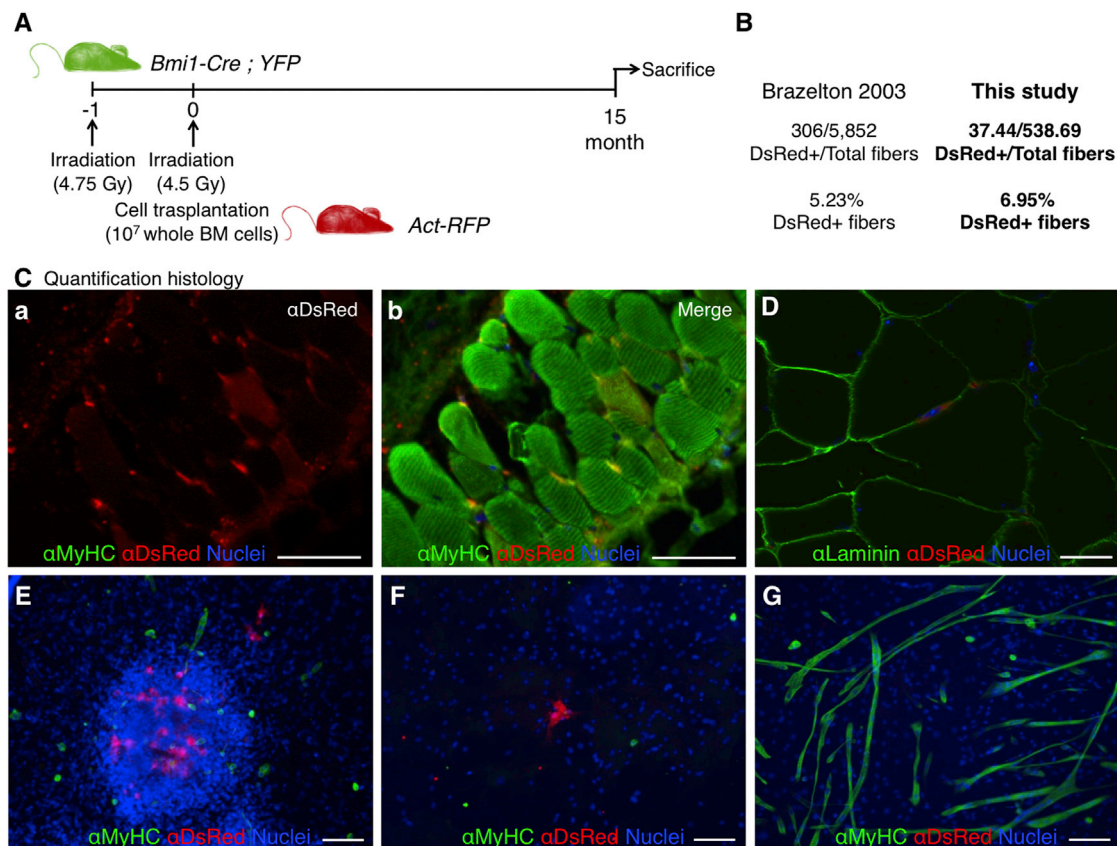


Figure 4. Contribution of Bone Marrow-Derived Cells to PC Fibers 15 Months after Bone Marrow Transplantation

(A) Outline of experimental design. Mice expressing YFP in *Bmi1*⁺ cell lineage were transplanted with RFP⁺ bone marrow (Valiente-Alandi et al., 2015).

(B) Quantification of DsRed-positive bone marrow-derived cell incorporation into PC in this study yielded results similar to those of Brazelton et al. (2003), i.e., higher than usual in vivo incorporation.

(C) Immunofluorescence detection of donor-derived RFP⁺ fibers with anti-DsRed and sarcoplasmic anti-myosin heavy-chain (MyHC, all fibers) antibodies showing the red channel (a) and the merged channels (b).

(D) Histological sections of dorsal skin showing a DsRed⁺ cell in a satellite cell position below Laminin⁺ basement membrane.

(E–G) The lack of contribution of bone marrow-derived cells to striated muscle differentiation in vitro was demonstrated by immunofluorescence with anti-DsRed and sarcoplasmic anti-myosin heavy-chain (MyHC, all fibers) antibodies. Nuclei were counterstained with Hoechst 33258 (blue).

Scale bars, 100 μ m.

status, we took advantage of the fact that robust striated muscle derivation (in vitro and in vivo) is obtained from dermis-derived sphere cultures (Garcia-Parra et al., 2014; Qiu et al., 2010; Wakabayashi et al., 2010). In fact, we previously hypothesized that those cultures expanded the PC satellite cells (Garcia-Parra et al., 2014). In vitro culture of dermal sphere cells from the RFP⁺ bone marrow-transplanted mice in myogenic conditions demonstrated no contribution of donor bone marrow cell progeny to the formed myotubes (Figures 4E–4G). These results indicated that cells of donor origin are capable of repopulating the muscle stem cell niche but may not fully acquire the relevant myogenic commitment. However, a better under-

standing of the process of myotube derivation from dermis-derived cultures was needed to ascertain their apparent loss of functionality.

PC Satellite Cell Progeny Is Enriched in Dermal Precursor Sphere Cultures

Because the identity of the myogenic cell in dermal precursor sphere cultures remains uncertain, we examined dermal spheres at the ultrastructural level by TEM (Figures 5A–5C). At day 7 of proliferation culture, two distinct cell subpopulations were observed: a majority of cells presented vacuoles (Figure 5A, black asterisks) while a second, minor population (10%–15%) did not (Figure 5A, white asterisks).

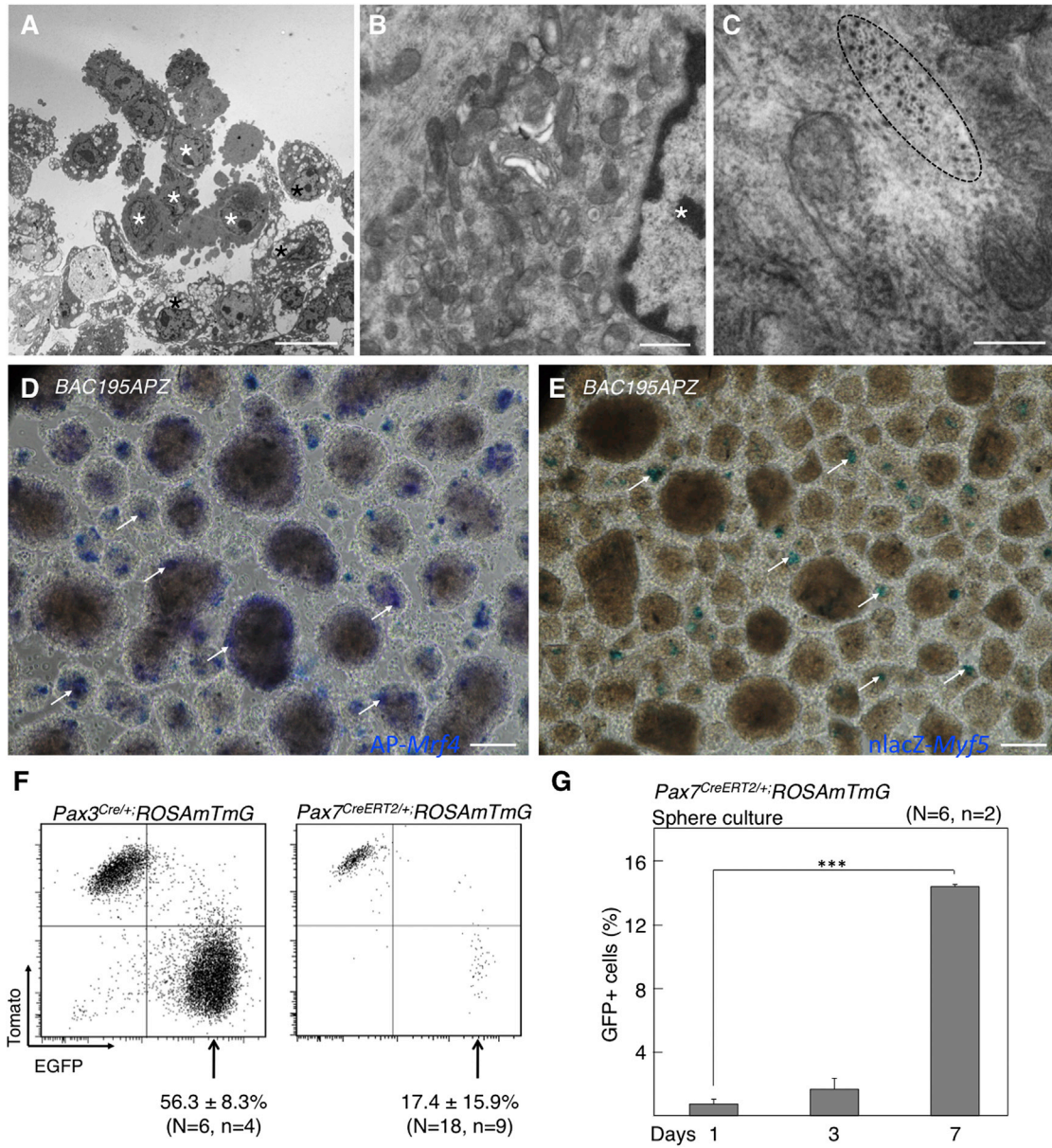


Figure 5. PC Satellite Cell Progeny Is Enriched in Dermal Precursor Sphere Cultures

(A–C) TEM images of dermal spheres. Cells with distinctive morphologies are marked by black and white asterisks. Actomyosin filaments are encircled in (C). (D and E) Detection of *AP-Mrf4*⁺ (D) and *nlacZ-Myf5*⁺ (E) cells in dermal sphere cultures. Positive cells are marked by arrows. (F) Flow cytometry analyses of mTomato- and mEGFP-expressing cells from *Pax3^{Cre}* and *Pax7^{CE}* mice. Data represent mean ± SD. The experiments were independently replicated as specified (N, mice; n, experiments). (G) Percentage of GFP⁺ cells by flow cytometry at 1, 3, and 7 days of dermosphere cultures. Bars represent means ± SD. ***p < 0.001. Scale bars represent 10 mm in (A), 500 nm in (B), 200 nm in (C), and 100 μm in (D) and (E). See also [Figures S3](#) and [S4](#).

Vacuole-rich cells had a phenotype consistent with immature fibroblasts (Figure 5B). In contrast, low-vacuole cells (white asterisks) were more rounded, had less heterochromatic nuclei, and presented abundant perinuclear mitochondria and undilated rough ER, consistent with a

myogenic fate (Mauro, 1961; Nag and Foster, 1981). Accordingly, actomyosin filaments could only be seen in the latter cells (Figure 5C).

To understand their origin and in vitro expansion, we analyzed dermal myogenic precursors in *B195APZ* mice



that express nLacZ and cytoplasmic AP driven by the full *Myf5* and *Mrf4* regulatory regions, respectively (Carvajal et al., 2001). At day 7 of proliferative culture, AP⁺ and β-Gal⁺ cells were detected in dermal spheres (Figures 5D and 5E; arrows). Furthermore, lineage-tracing studies of *Pax3*⁺ and *Pax7*⁺ cells demonstrated their presence in dermal sphere cultures (Figure 5F; but see below with regard to *Pax3*⁺ cells). To test for a possible enrichment of PC satellite-derived cells during sphere culture, we used the inducible *Pax7* mouse model and quantified *Pax7*⁺ cells at different times of sphere proliferation (Figure 5G). There was at least 15-fold enrichment in the proportion of GFP (*Pax7*)⁺ cells in the 7 days of sphere culture, indicating that dermal myogenic precursors have an advantage over other sphere cells in survival and/or proliferation rates. We also looked at the capacity for myotube derivation of PC-derived satellite cells compared with limb muscle (tibialis anterior [TA])-derived cells (Figure S3A). For this comparison, it must be taken into account that the vast amount of non-myogenic cells in dermis-derived cultures dilutes the number of PC satellite cells, which is about 15% at day 7 of proliferation culture (Figure 5G). In contrast, the number of satellite cells in myspheres is much greater (about 70% [Sarig et al., 2006]). Real-time qPCR analysis for mRNA expression of myogenic genes showed a significant (approximately 3-fold) upregulation of myogenic genes in differentiated cultures from TA compared with PC (Figure S3B), which indicates that PC-derived satellite cells have a myogenic capacity similar to that of TA-derived satellite cells. Finally, the contribution of PC satellite cells to myotubes was quantified in differentiation culture. The percentage of mono- and multinucleated cells derived from the *Pax7*⁺ lineage was quantified at days 1, 3, and 7 of differentiation, demonstrating significant incorporation of GFP⁺ cells into the developing myotubes (Figure S3C). In summary, a significant enrichment of PC satellite cell progeny that retained myogenic capacity was detected in dermis-derived sphere cultures.

PC Satellite Cell Progeny Is the Only Cell Population Responsible for Dermis-Derived Myogenesis In Vitro

Dermis-derived sphere cultures are highly heterogeneous (Etxaniz et al., 2014). To confirm the identity of the myogenic progenitor, we placed dermal spheres (unsorted cultures) into striated muscle differentiation conditions (Figure S4). After 7-day unsorted differentiation culture of *BAC195APZ* spheres, all myotubes were *Mrf4*(AP)⁺ (Figure S4A). *Myf5*(β-Gal)⁺ cells appeared as mononucleated myoblasts or juxtaposed to differentiating myotubes (Figure S4B). Lineage tracing of the *Myf5Cre^{Sor}*, *Pax3^{Cre/+}*, *B195AP-Cre*, and *Pax7^{CreERT2/+}* constructs showed in all cases a contribution of these cell lineages to dermis-derived myotubes (Figures S4C–S4F). Importantly, no MyHC⁺ myo-

tubes negative for any of the reporter genes were detected, indicating that they all derived from PC satellite cells.

To study whether perivascularly localized cells present in the dermis or PC muscle also contribute to striated muscle derivation, we traced the perivascular cells by chondroitin sulfate proteoglycan 4 (*Cspg4*, coding for NG2) expression (Figure S4G). This construct traced interstitial cells within the PC muscle (Figure S4Ga) that did not give EYFP⁺ myotubes in unsorted cultures (Figure S4Gb) or after sorting of positive and negative EYFP fractions (Figures S4Gc and S4Gd). To analyze this in a more quantitative manner, mRNA was extracted from fluorescence-activated cell sorting (FACS)-sorted cell fractions and the relative expression of myogenic genes was quantified by qRT-PCR (Figure S4Ge). As expected, the myogenic marker mRNAs were preferentially upregulated in the *Cspg4*[−] cell fraction, indicating no contribution of perivascular cells to dermal myogenesis.

To confirm the contribution of PC satellite cells to dermal myogenesis, we sorted by FACS the positive and negative cell populations in *Myf5Cre^{Sor}*, *Pax3^{GFP/+}*, *B195AP-Cre*, and *Pax7^{CreERT2/+}* constructs (Figure 6). MyHC⁺ myotubes appeared only in the marker-positive cell fractions (Figures 6A–6C), as confirmed by the relative expression of myogenic genes by qRT-PCR (Figure S5). Of note, *Pax3*⁺ dermal precursor cells are detected as GFP^{low} cells in *Pax3^{GFP/+}* mice (Djian-Zaouche et al., 2012) (Figure 6Da). Dermal GFP[−], GFP^{low}, and GFP^{high} cell fractions of *Pax3^{GFP/+}* mice were isolated and only the GFP[−] cell fraction generated myotubes, with no contribution of dermal precursor (GFP^{low}) cells to the myogenic differentiation (Figures 6Db–6Dd). These data suggested that dermal myogenic precursors derive from *Myf5*⁺ *Pax3/Pax7*⁺ satellite cells of the PC. To further substantiate this claim, transcriptomic analyses were performed and, once again, the results suggested that dermal myogenic precursor cells were of muscle origin (Figures S6 and S7 and accompanying description).

Ablation of PC Satellite Cells Abrogates Dermis-Derived Myogenesis In Vitro

The previous results strongly suggested that distinct dermal precursors, possibly PC satellite cells, were responsible for dermis-derived myogenesis. To unambiguously demonstrate the origin of dermal myogenic precursors, we specifically ablated PC satellite cells in vivo through crossing the *Pax7^{CreERT2/+}* construct with *R26R^{GFP-DTA/+}* mice (Ivanova et al., 2005). Upon TMX-mediated *Cre* induction (Figure 6E), diphtheria toxin fragment A (DTA) expression is activated in these mice, resulting in specific ablation of the *Pax7*⁺ cell lineage. As expected, DTA-mediated ablation of the *Pax7*⁺ cells resulted in no MyHC⁺ myotube formation (Figures 6F–6I). Overall, these results demonstrated

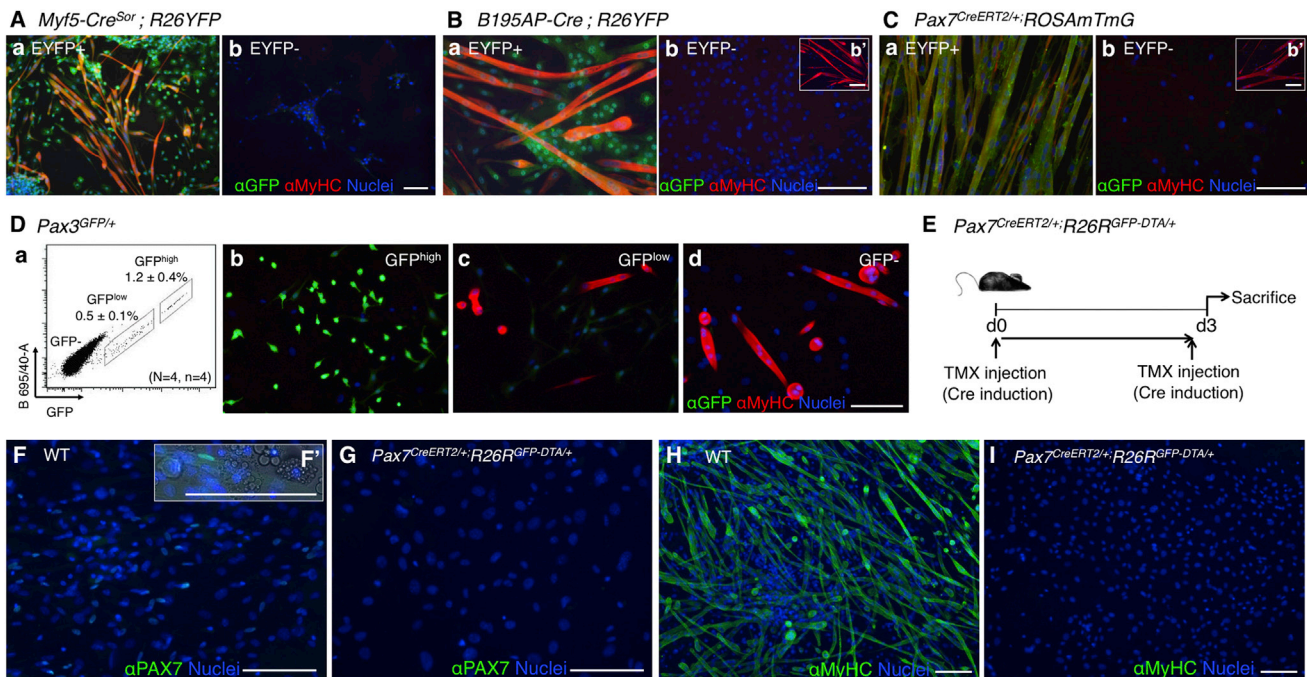


Figure 6. Ablation of Muscle Satellite Cells In Vivo Abrogates In Vitro Dermis-Derived Myotube Formation

(A–C) Contribution of FACS-sorted cell fractions of *Myf5*^{SOR} (A) (EYFP⁺ [a], EYFP⁻ [b]), *B195AP* (B) (EYFP⁺ [a], EYFP⁻ [b]), and *Pax7*^{CE} (C) (EYFP⁺ [a], EYFP⁻ [b]) to striated muscle differentiation was measured by immunofluorescence with anti-GFP (for EYFP expression) and sarcofleming anti-myosin heavy-chain (MyHC, all fibers) antibodies.

(D) Flow cytometry analysis of dermal spheres in *Pax3*^{GFP/+} mice (a) showed two distinct cell populations according to GFP expression levels. Data represent mean \pm SD (N, mice; n, experiments). (b–d) Contribution of FACS-sorted cell fractions (GFP^{high} [b], GFP^{low} [c], and GFP⁻ [d]) to striated muscle differentiation was measured by immunofluorescence with anti-GFP and sarcoplasmic anti-myosin heavy-chain (MyHC, all fibers) antibodies.

(E) Outline of experimental design. d, day.

(F–I) Contribution of wild-type (WT) and *Pax7*^{CE-DTA}-derived cells to striated muscle differentiation was measured by immunofluorescence with anti-PAX7 (F and G; higher-magnification inset in F'), and sarcoplasmic anti-myosin heavy-chain (MyHC, all fibers) (H and I) antibodies. Nuclei were counterstained with Hoechst 33258 (blue).

Scale bars, 100 μ m. See also [Figures S5–S7](#).

that dermis-derived myogenesis originates from the PC satellite cell population.

In Vivo Contribution of *B195AP*⁺ Cells to Injury-Induced Skeletal Muscle Regeneration

Dermis-derived precursor cells are able to engraft into injured skeletal muscle (both after freeze-crush injury and cardiotoxin [CTX]-induced damage) and survive up to 20 weeks post injection ([Qiu et al., 2010](#); [Wakabayashi et al., 2010](#)). To confirm that *Myf5*⁺ dermal cells were myogenic in vivo ([Figure 7](#)), we injected unsorted dermal cells of the *B195AP-Cre* model crossed with *R26YFP* in the CTX injury model ([Figure 7A](#)). One week after injection, one out of three mice injected with *B195AP*⁺ cells showed 28 ± 3 EYFP⁺ regenerated myofibers, while in the other two no EYFP⁺ fiber was detected ([Figure 7B](#) and data not shown). Most EYFP⁺ cells localized in the interstitial spaces

of skeletal muscle and a minority was positioned underneath the basement membrane, suggesting repopulation of the satellite cell compartment. Therefore, PC satellite cell-derived *B195AP*⁺ cells were able to regenerate injured skeletal muscle and thus might represent the in vivo myogenic cell population that had been previously described in the mouse dermis.

DISCUSSION

An important barrier for the use of satellite cells in regenerative medicine, for instance in the field of muscular dystrophies, is the lack of understanding of how to maintain isolated satellite cells in culture such that they are of therapeutic use ([Aziz et al., 2012](#)). The PC muscle seems to have high regenerative activity ([Brazelton et al., 2003](#)) and is not

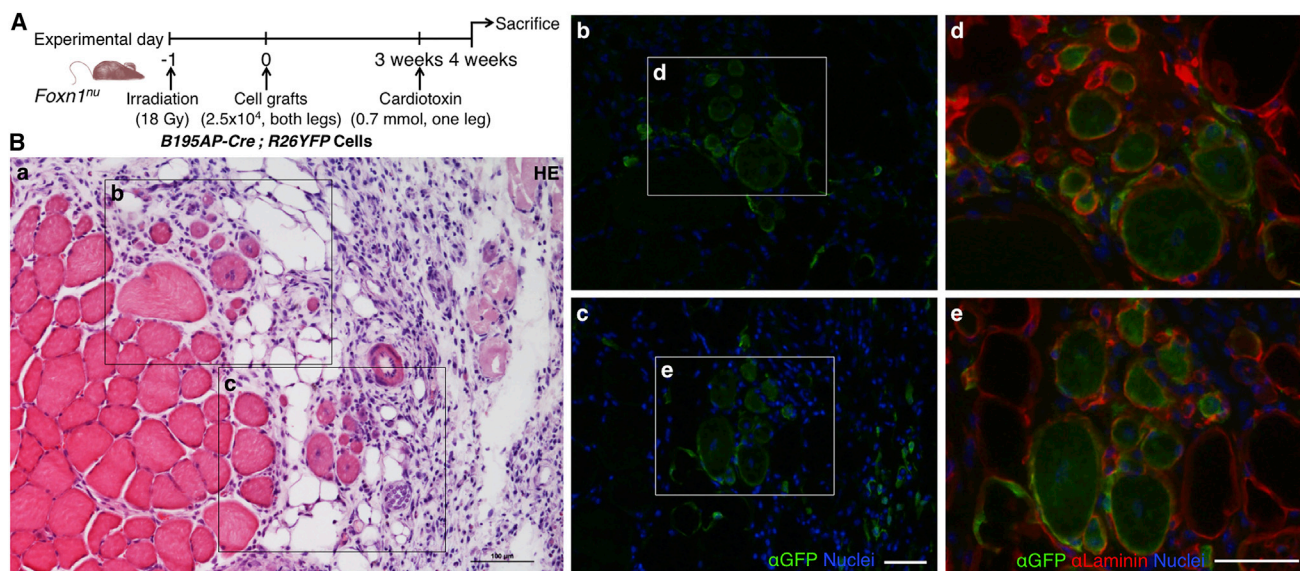


Figure 7. In Vivo Contribution from *B195AP*⁺ Cells to Striated Muscle Regeneration

(A) Outline of experimental design.

(B) Histological analysis of the in vivo regenerative potential of grafted cells. (a) Tibialis anterior muscle section stained with H&E showing the localization of the other panels. (b and c) Regenerative muscle fibers, defined by centrally located nuclei (blue), showed EYFP expression, as detected with anti-GFP antibody (green). (d and e) Higher-magnification pictures of EYFP⁺ myofibers (green) and Laminin (red). Nuclei were counterstained with Hoechst 33258 (blue). Scale bars, 100 μm .

only accessible but also dispensable and, as such, can be repeatedly biopsied. For these reasons the PC may be considered as a good muscle for the study of satellite cell biology. In this article we unravel unique aspects of PC muscle biology and describe the origin and role of satellite cells upon skin and muscle wounding.

In response to full-thickness skin wounding, we show an increase in muscle regeneration but no contribution of the *Pax7*-derived cell lineage to the myofibroblasts in the wound bed. This is relevant because a putative role of PC muscle in facilitating the rapid healing (by second intention) observed in rodents has been hypothesized (Greenwood, 2010; Volk and Bohling, 2013). At the wound edge, skNAC, a factor regulating postnatal muscle regeneration (Park et al., 2010), is upregulated in the adjacent PC fibers (Munz et al., 1999), and Tap63⁺ cells appear in both the PC and newly formed granulation tissue (Bamberger et al., 2005). Tap63 has been linked to dermal stem cell function (Su et al., 2009), and contraction of the granulation tissue supports rapid healing (Billingham and Medawar, 1955; Brunius et al., 1968; Watts et al., 1958). Our lineage-tracing data demonstrate no contribution of *Pax7*⁺ lineage-derived cells, i.e., activated satellite cells or components of the regenerated myofibers into the granulation tissue, although we cannot discard the contribution from other cell lineages present in PC muscle. In the TA muscle irradiation/CTX model, which is a

more standardized muscle injury model, we see that the dermis-derived cells are able to regenerate myofibers, as expected for transplanted satellite cells in such a model.

Previous reports had shown an increased contribution of bone marrow-derived cells (possibly HSCs) to PC muscle (Brazelton et al., 2003; Corbel et al., 2003). This incorporation is unique in that it is highly divergent to other muscle groups (Camargo et al., 2003; Ferrari et al., 1998, 2001; Ferrari and Mavilio, 2002; Sherwood et al., 2004a; Sherwood et al., 2004b; Wagers et al., 2002). However, the donor bone marrow cells, even if able to engraft into the PC satellite cell niche, were unable to generate myotubes from dermis-derived sphere cultures. This may be due to several reasons, but it is tempting to speculate that the engrafted cells failed to reach full conversion to the satellite cell fate, as previously shown in other systems (Cossu, 2004; Lapidus et al., 2004). The relevance of circulating HSC fusion into heart and skeletal muscle are unclear, but the phenomenon keeps arising in the literature (Quijada and Sussman, 2015), and occurs also in human muscle (Stromberg et al., 2013). Based on these results we propose the PC as the most appropriate system to further understand the role of mobilized cells that engraft in skeletal muscle, a research area that has been neglected possibly because of the extreme rarity of the fusion events in the muscle groups that are most often analyzed. Determining the identity of the homing factor(s) that facilitate an



increased engraftment of mobilized cells into the PC in comparison with other skeletal muscles might be exploited for therapeutic use (Asakura, 2012). Potential candidates include the SDF-1/CXCR4 axis (Cheng et al., 2015), although it is important to note that as the PC is signaling for mobilized cell engraftment in the absence of injury, the nature of the signal might be different.

Regarding the developmental origin of PC satellite cells, we have shown that this muscle is no different to other trunk muscles in that it originates from *Myf5*⁺, *Pax3*/*Pax7*⁺ progenitors. This will help in respect of comparability with studies performed in satellite cells from other trunk muscles. Finally, for many years it has been known that a small population of dermal cells, of unknown origin, presents myogenic properties (reviewed by White and Grounds, 2003). Our results unequivocally demonstrate that PC satellite cells are the myogenic precursor cells of murine dermis. The present article and other recent data showing that dermis-derived neural stem cells arise from the Schwann cell lineage (Etzaniz et al., 2014; Gresset et al., 2015) urge us to interpret with caution some of the multipotency wrongly attributed to tissue-resident precursors.

EXPERIMENTAL PROCEDURES

Mouse Strains

Eight-week-old mice were used in all experiments. Strains used are detailed in Table S1. Animal experimentation was approved by Biodonostia Animal Care Committee (San Sebastian, Spain) in accordance with Spanish Royal Decree 53/2013, European Directive 2010/63/EU and other relevant guidelines.

Pax7^{CE};*ROSAmTmG* Induction by Tamoxifen Injection

Pax7^{CE/+} mice and control (*ROSAmTmG*^{+/-}) littermates were intraperitoneally injected (2.5 μ L/g mouse) with 20 mg/mL TMX (T5648, Sigma-Aldrich) diluted in corn oil (C8267, Sigma-Aldrich) (Dellavalle et al., 2011), for 3 days at postnatal days 14 (P14), P16, and P35, and euthanized at 7–8 weeks.

Skin Punch

Pax7^{CreERT2/+};*ROSAmTmG* and control *ROSAmTmG* adult mice were intraperitoneally injected with 2 mg TMX for five consecutive days, 4 weeks before injury, or during the first five days of muscle regeneration. Following general anesthesia, the mouse's dorsal skin was shaved and cleaned with povidone and alcohol 70% before proceeding with the skin punch. Full-thickness wounds extended to the depth of the superficial fascia (removing the PC) on either side of the midline were made with a dermal biopsy punch (4 mm diameter; Stiefel) (Wang et al., 2013). By holding the skin with forceps the skin was pushed to one side to avoid damage to back muscles, and two holes were punched simultaneously. The recovered skin was frozen as a control for histological or RNA

analysis. The wounds were protected with a sheet of sterile gauze (Tegaderm 4 \times 4 cm) kept until the end of the experiment. Buprenorphine painkiller (Vetergesic 0.3 mg/mL; Soceval) was injected directly after the surgery and again 4–6 hr later, and on the next day. Mice were placed individually in cages allowing free access to food and water ad libitum. After wounding, animals were carefully monitored to avoid infection and suffering. Skins were finally recovered 5 and 10 days after injury. As controls, uninjured skins from the same animals were taken (n = 3 animals per condition).

Isolation, Proliferation, and Striated Muscle Differentiation of Dermal Precursor Cells

Precursor cells were isolated from dorsal back skin and imaged by fluorescence as described by García-Parra et al. (2012). Dermal sphere expansion was performed in proliferation medium (Neurobasal A [Gibco] supplemented with 2% B27 [Gibco], 200 mM 1% L-glutamine [Sigma-Aldrich], and 1% penicillin/streptomycin, supplemented with 2% low serum growth supplement [Gibco], 40 ng/mL epidermal growth factor [R&D Systems], and 80 ng/mL basic fibroblast growth factor [FGF2; R&D]). For differentiation, extracellular matrix-coated glass coverslips were prepared as described by Garcia-Parra et al. (2014). Primary spheres were gently disaggregated with a 0.25% trypsin-EDTA solution (Sigma-Aldrich) and resuspended in proliferation medium without added growth factors plus 10% fetal bovine serum (ATCC), before plating onto coated coverslips at a density of 80,000 cells/cm². Every 2 days, half of the medium was replenished.

Depletion of Dermal Satellite Cells

Pax7^{CreERT2/+};*R26R*^{GFP-DTA/+} and control *R26R*^{GFP-DTA/+} mice were intraperitoneally injected with 10 mg TMX as previously described (Lepper et al., 2011). Forty-eight hours later, dorsal skins were recovered for sphere culture, and TA and soleus muscles frozen for histological and RNA analysis (n = 3 animals per condition).

In Vivo Cell Grafting and Muscle Injury

Primary dermospheres at day 7 of proliferation were gently disaggregated with a 0.25% trypsin-EDTA solution (Sigma-Aldrich) and resuspended in PBS. Muscle damage experiments were done according to Boldrin et al. (2012) and Boldrin et al. (2009). Ten-week-old nude *Foxn1*tm mice were anesthetized and both hind limbs were irradiated with 18 Gy at a dose rate of 300 cGy/min. One day later, mice were anesthetized with isoflurane and received 2.5×10^4 unsorted *Myf5Cre*^{SOR};*R26YFP* (pooled from n = 3 mice) or *B195AP-Cre*;*R26YFP* (n = 3 mice) cells into both TA muscles using a 26-gauge Hamilton syringe. Three weeks after transplantation, right TA muscles of anesthetized host mice were injected with 0.7 mmol cardiotoxin (Sigma, C9759) while PBS was administered to the contralateral muscle. Controls were age-matched mice that were non-irradiated and received PBS. Engrafted muscles were removed 4 weeks after cell injection and processed for histological analysis. Seven-micrometer serial transverse cryosections were cut at intervals of 100 μ m throughout the entire muscles. Sections were stained with H&E and by immunofluorescence staining using antibodies as detailed in Supplemental Experimental Procedures. The mean number of donor origin regenerated myofibers was



calculated by counting the number of EYFP⁺ centrally nucleated fibers in three intervals of 100- μ m serial sections.

Assessment of Statistical Significance

Statistical analysis was conducted using GraphPad Prism software. A one-way ANOVA with subsequent pairwise multiple comparison procedures (Bonferroni's test) was used to assess statistical significance of the results from qRT-PCR experiments. Student's t test was used to assess statistical significance of the results from Pax7(GFP)⁺ cell quantification experiments. Asterisks in figures represent statistical significance of * $p < 0.05$, ** $p < 0.01$, or *** $p < 0.001$.

ACCESSION NUMBERS

Transcriptomic data of dermal cell fractions are deposited in NCBI's Gene Expression Omnibus (Edgar et al., 2002) under accession number GEO: GSE67693.

SUPPLEMENTAL INFORMATION

Supplemental Information includes Supplemental Results, Supplemental Experimental Procedures, seven figures, and two tables and can be found with this article online at <http://dx.doi.org/10.1016/j.stemcr.2016.08.002>.

AUTHOR CONTRIBUTIONS

N.N.G. performed most of the experimental work, with the help of M.G., J.L., and P.G.P. C.S.J. helped perform in vivo cell transplantation experiments. S.A.M. and F.R. were responsible for inducible Pax7 lineage-tracing experiments. A.A. performed qRT-PCR analyses. J.J.C. generated B195AP-Cre-expressing mice and together with M.L.M. characterized this transgenic line. P.G.B. and J.M.G.V. performed ultrastructural analyses. L.T., V.A.L., and M.J.A.B. did the transcriptomics and their corresponding analyses, respectively. D.H. and A.B. performed bone marrow transplantation experiments. A.M. and A.L.M. provided helpful guidance, reagents, and suggestions. N.N.G. and A.I. wrote the manuscript, which was approved by all authors prior to submission. P.G.P. and A.I. directed all experimental work.

ACKNOWLEDGMENTS

We thank investigators for monoclonal antibodies A4.1025 (H.M. Blau) and F5D (W.E. Wright), which were obtained from the Developmental Studies Hybridoma Bank (developed under the auspices of the NICHD and maintained by The University of Iowa, Department of Biology, Iowa City, IA). Special thanks to G. Cossu for critical reading of the manuscript. We are also grateful to F. Costantini, C.-M. Fan, C. Lepper, M.J. Sánchez-Sanz, H. Sakai, and S. Tajbakhsh for kindly providing study materials; S. Lamarre of the GeT-Biochip facility for help in the microarray data; D. Ortiz de Urbina, J.C. Mazabuel, and A. Guisasaola for help with irradiation protocol; and A. Aduriz, A. Pavón, and M. P. López-Mato for help with FACS analyses. This work was supported by grants from Instituto de Salud Carlos III (ISCIII; PS09/00660, PI13/02172, and PI14/7436), Gobierno Vasco (SAIO12-PE12BN008) from Spain and the European Union (POCTEFA-INTERREG IV A program; REF BIO13/BIOD/006

and REF BIO13/BIOD/009). N.N.G. received a studentship from the Department of Education, University and Research of the Basque Government (PRE2013-1-1168). P.G.P. received fellowships from the Department of Health of the Basque government (2013011016), EMBO (Short-Term; ASTF 542–2013), and Boehringer Ingelheim Fonds. M.L.M. and J.J.C. were supported by a Marie Curie Career Integration Grant from the European Commission (PEOPLE-CIG/1590). A.I. was supported by the Programa I3SNS (CES09/015) from ISCIII and by Osakidetza-Servicio Vasco de Salud (Spain). M.G. and S.A.M. contributed equally to this work.

Received: April 7, 2015

Revised: August 1, 2016

Accepted: August 1, 2016

Published: September 1, 2016

REFERENCES

- Asakura, A. (2012). Skeletal muscle-derived hematopoietic stem cells: muscular dystrophy therapy by bone marrow transplantation. *J. Stem Cell Res Ther. (Suppl 11)*, 005.
- Atit, R., Sgaier, S.K., Mohamed, O.A., Taketo, M.M., Dufort, D., Joyner, A.L., Niswander, L., and Conlon, R.A. (2006). Beta-catenin activation is necessary and sufficient to specify the dorsal dermal fate in the mouse. *Dev. Biol.* 296, 164–176.
- Aziz, A., Sebastian, S., and Dilworth, F.J. (2012). The origin and fate of muscle satellite cells. *Stem Cell Rev.* 8, 609–622.
- Bamberger, C., Hafner, A., Schmale, H., and Werner, S. (2005). Expression of different p63 variants in healing skin wounds suggests a role of p63 in reepithelialization and muscle repair. *Wound Repair Regen.* 13, 41–50.
- Billingham, R.E., and Medawar, P.B. (1955). Contracture and intussusceptive growth in the healing of extensive wounds in mammalian skin. *J. Anat.* 89, 114–123.
- Biressi, S., Bjornson, C.R., Carlig, P.M., Nishijo, K., Keller, C., and Rando, T.A. (2013). Myf5 expression during fetal myogenesis defines the developmental progenitors of adult satellite cells. *Dev. Biol.* 379, 195–207.
- Boldrin, L., Zammit, P.S., Muntoni, F., and Morgan, J.E. (2009). Mature adult dystrophic mouse muscle environment does not impede efficient engrafted satellite cell regeneration and self-renewal. *Stem Cells* 27, 2478–2487.
- Boldrin, L., Neal, A., Zammit, P.S., Muntoni, F., and Morgan, J.E. (2012). Donor satellite cell engraftment is significantly augmented when the host niche is preserved and endogenous satellite cells are incapacitated. *Stem Cells* 30, 1971–1984.
- Brazelton, R., Nystrom, M., and Blau, H. (2003). Significant differences among skeletal muscles in the incorporation of bone marrow-derived cells. *Dev. Biol.* 262, 64–74.
- Brunius, U., Zederfeldt, B., and Ahren, C. (1968). Healing of skin incisions with intact subcutaneous muscle closed by non-suture technique. A tensiometric and histologic study in the rat. *Acta Chir. Scand.* 134, 187–193.
- Buckingham, M., and Rigby, P.W.J. (2014). Gene regulatory networks and transcriptional mechanisms that control myogenesis. *Dev. Cell* 28, 225–238.



- Camargo, F.D., Green, R., Capetanaki, Y., Jackson, K.A., and Goodell, M.A. (2003). Single hematopoietic stem cells generate skeletal muscle through myeloid intermediates. *Nat. Med.* *9*, 1520–1527.
- Carvajal, J.J., Cox, D., Summerbell, D., and Rigby, P.W.J. (2001). A BAC transgenic analysis of the *Mrf4/Myf5* locus reveals interdigitated elements that control activation and maintenance of gene expression during muscle development. *Development* *186*, 1857–1868.
- Cheng, M., Huang, K., Zhou, J., Yan, D., Tang, Y.L., Zhao, T.C., Miller, R.J., Kishore, R., Losordo, D.W., and Qin, G. (2015). A critical role of Src family kinase in SDF-1/CXCR4-mediated bone marrow progenitor cell recruitment to the ischemic heart. *J. Mol. Cell Cardiol.* *81*, 49–53.
- Corbel, S.Y., Lee, A., Yi, L., Duenas, J., Brazelton, T.R., Blau, H.M., and Rossi, F.M. (2003). Contribution of hematopoietic stem cells to skeletal muscle. *Nat. Med.* *9*, 1528–1532.
- Cossu, G. (2004). Fusion of bone marrow-derived stem cells with striated muscle may not be sufficient to activate muscle genes. *J. Clin. Invest.* *114*, 1540–1543.
- Dellavalle, A., Maroli, G., Covarello, D., Azzoni, E., Innocenzi, A., Perani, L., Antonini, S., Sambasivan, R., Brunelli, S., Tajbakhsh, S., et al. (2011). Pericytes resident in postnatal skeletal muscle differentiate into muscle fibres and generate satellite cells. *Nat. Commun.* *2*, 499.
- DiMario, J.X., Uzman, A., and Strohman, R.C. (1991). Fiber regeneration is not persistent in dystrophic (MDX) mouse skeletal muscle. *Dev. Biol.* *148*, 314–321.
- Djian-Zaouche, J., Campagne, C., Reyes-Gomez, E., Gadin-Czerw, S., Bernex, F., Louise, A., Relaix, F., Buckingham, M., Panthier, J.J., and Aubin-Houzelstein, G. (2012). Pax3(GFP), a new reporter for the melanocyte lineage, highlights novel aspects of PAX3 expression in the skin. *Pigment Cell Melanoma Res.* *25*, 545–554.
- Edgar, R., Domrachev, M., and Lash, A.E. (2002). Gene Expression Omnibus: NCBI gene expression and hybridization array data repository. *Nucleic Acids Res.* *30*, 207–210.
- Eppig, J.T., Blake, J.A., Bult, C.J., Kadin, J.A., and Richardson, J.E. (2015). The Mouse Genome Database (MGD): facilitating mouse as a model for human biology and disease. *Nucleic Acids Res.* *43*, D726–D736.
- Etzaniz, U., Perez-San Vicente, A., Gago-Lopez, N., Garcia-Dominguez, M., Iribar, H., Aduriz, A., Perez-Lopez, V., Burgoa, I., Irizar, H., Munoz-Culla, M., et al. (2014). Neural-competent cells of adult human dermis belong to the Schwann lineage. *Stem Cell Rep.* *3*, 774–788.
- Ferrari, G., and Mavilio, F. (2002). Myogenic stem cells from the bone marrow: a therapeutic alternative for muscular dystrophy? *Neuromuscul. Disord.* *12 (Suppl 1)*, S7–S10.
- Ferrari, G., Cusella-De Angelis, G., Coletta, M., Paolucci, E., Stornaiuolo, A., Cossu, G., and Mavilio, F. (1998). Muscle regeneration by bone marrow-derived myogenic progenitors. *Science* *279*, 1528–1530.
- Ferrari, G., Stornaiuolo, A., and Mavilio, F. (2001). Failure to correct murine muscular dystrophy. *Nature* *411*, 1014–1015.
- García-Parra, P., Cavaliere, F., Maroto, M., Bilbao, L., Obieta, I., López de Munain, A., Alava, J.I., and Izeta, A. (2012). Modeling neural differentiation on micropatterned substrates coated with neural matrix components. *Front. Cell Neurosci.* *6*, 10.
- García-Parra, P., Naldaiz-Gastesi, N., Maroto, M., Padin, J.F., Goicoechea, M., Aiastui, A., Fernandez-Morales, J.C., Garcia-Belda, P., Lacalle, J., Alava, J.I., et al. (2014). Murine muscle engineered from dermal precursors: an in vitro model for skeletal muscle generation, degeneration, and fatty infiltration. *Tissue Eng. Part C Methods* *20*, 28–41.
- Gayraud-Morel, B., Chretien, F., Jory, A., Sambasivan, R., Negroni, E., Flamant, P., Soubigou, G., Coppee, J.Y., Di Santo, J., Cumanò, A., et al. (2012). Myf5 haploinsufficiency reveals distinct cell fate potentials for adult skeletal muscle stem cells. *J. Cell Sci.* *125*, 1738–1749.
- Greenwood, J.E. (2010). Function of the panniculus carnosus—a hypothesis. *Vet. Rec.* *167*, 760.
- Gresset, A., Couplier, F., Gerschenfeld, G., Jourdon, A., Matesic, G., Richard, L., Vallat, J.M., Charnay, P., and Topilko, P. (2015). Boundary caps give rise to neurogenic stem cells and terminal glia in the skin. *Stem Cell Rep.* *5*, 278–290.
- Gros, J., Manceau, M., Thome, V., and Marcelle, C. (2005). A common somitic origin for embryonic muscle progenitors and satellite cells. *Nature* *435*, 954–958.
- Hughes, A.F.W., and Dann, L. (1941). Vascular regeneration in experimental wounds and burns. *Br. J. Exp. Pathol.* *22*, 9–14.
- Ivanova, A., Signore, M., Caro, N., Greene, N.D., Copp, A.J., and Martinez-Barbera, J.P. (2005). In vivo genetic ablation by Cre-mediated expression of diphtheria toxin fragment A. *Genesis* *43*, 129–135.
- Kassar-Duchossoy, L., Gayraud-Morel, B., Gomes, D., Rocancourt, D., Buckingham, M., Shinin, V., and Tajbakhsh, S. (2004). *Mrf4* determines skeletal muscle identity in *Myf5:Myod* double-mutant mice. *Nature* *431*, 466–471.
- Kassar-Duchossoy, L., Giaccone, E., Gayraud-Morel, B., Jory, A., Gomès, D., and Tajbakhsh, S. (2005). Pax3/Pax7 mark a novel population of primitive myogenic cells during development. *Genes Dev.* *19*, 1426–1431.
- Kuang, S., Kuroda, K., Grand, F.L., and Rudnicki, M. (2007). Asymmetric self-renewal and commitment of satellite stem cells in muscle. *Cell* *129*, 999–1010.
- Lapidos, K.A., Chen, Y.E., Earley, J.U., Heydemann, A., Huber, J.M., Chien, M., Ma, A., and McNally, E.M. (2004). Transplanted hematopoietic stem cells demonstrate impaired sarcoglycan expression after engraftment into cardiac and skeletal muscle. *J. Clin. Invest.* *114*, 1577–1585.
- Lepper, C., and Fan, C.-m. (2011). Inducible lineage tracing of Pax7-descendant cells reveals embryonic origin of adult satellite cells. *Genesis* *48*, 424–436.
- Lepper, C., Partridge, T.a., and Fan, C.-M. (2011). An absolute requirement for Pax7-positive satellite cells in acute injury-induced skeletal muscle regeneration. *Development* *138*, 3639–3646.
- Mauro, A. (1961). Satellite cell of skeletal muscle fibers. *J. Biophys. Biochem. Cytol.* *9*, 493–495.
- McDonald, T.A., Zepeda, M.L., Tomlinson, M.J., Bee, W.H., and Ivens, I.A. (2010). Subcutaneous administration of biotherapeutics: current experience in animal models. *Curr. Opin. Mol. Ther.* *12*, 461–470.



- Munz, B., Wiedmann, M., Lochmuller, H., and Werner, S. (1999). Cloning of novel injury-regulated genes. Implications for an important role of the muscle-specific protein skNAC in muscle repair. *J. Biol. Chem.* *274*, 13305–13310.
- Nag, A.C., and Foster, J.D. (1981). Myogenesis in adult mammalian skeletal muscle in vitro. *J. Anat.* *132*, 1–18.
- Novakov, S.S., Yotova, N.I., Petleshkova, T.D., and Muletarov, S.M. (2008). Sternalis muscle—a riddle that still awaits an answer short communication. *Folia Med.* *50*, 63–66.
- Park, C.Y., Pierce, S.A., von Drehle, M., Ivey, K.N., Morgan, J.A., Blau, H.M., and Srivastava, D. (2010). skNAC, a Smyd1-interacting transcription factor, is involved in cardiac development and skeletal muscle growth and regeneration. *Proc. Natl. Acad. Sci. USA* *107*, 20750–20755.
- Qiu, Z., Miao, C., Li, J., Lei, X., Liu, S., Guo, W., Cao, Y., and Duan, E.K. (2010). Skeletal myogenic potential of mouse skin-derived precursors. *Stem Cells Dev.* *19*, 259–268.
- Quijada, P., and Sussman, M.A. (2015). Circulating around the tissue: hematopoietic cell-based fusion versus transdifferentiation. *Circ. Res.* *116*, 563–565.
- Randolph, M.E., and Pavlath, G.K. (2015). A muscle stem cell for every muscle: variability of satellite cell biology among different muscle groups. *Front. Aging Neurosci.* *7*, 190.
- Relaix, F., Rocancourt, D., Mansouri, A., and Buckingham, M. (2005). A Pax3/Pax7-dependent population of skeletal muscle progenitor cells. *Nature* *435*, 948–953.
- Robson, L.G., Di Foggia, V., Radunovic, A., Bird, K., Zhang, X., and Marino, S. (2011). *Bmi1* is expressed in postnatal myogenic satellite cells, controls their maintenance and plays an essential role in repeated muscle regeneration. *PLoS One* *6*, e27116.
- Sarig, R., Baruchi, Z., Fuchs, O., Nudel, U., and Yaffe, D. (2006). Regeneration and transdifferentiation potential of muscle-derived stem cells propagated as myospheres. *Stem Cells* *24*, 1769–1778.
- Schiaffino, S., Rossi, A.C., Smerdu, V., Leinwand, L.A., and Reggiani, C. (2015). Developmental myosins: expression patterns and functional significance. *Skeletal Muscle* *5*, 22.
- Schienda, J., Engleka, K.A., Jun, S., Hansen, M.S., Epstein, J.A., Tabin, C.J., Kunkel, L.M., and Kardon, G. (2006). Somitic origin of limb muscle satellite and side population cells. *Proc. Natl. Acad. Sci. USA* *103*, 945–950.
- Sherwood, R.I., Christensen, J.L., Conboy, I.M., Conboy, M.J., Rando, T.A., Weissman, I.L., and Wagers, A.J. (2004a). Isolation of adult mouse myogenic progenitors: functional heterogeneity of cells within and engrafting skeletal muscle. *Cell* *119*, 543–554.
- Sherwood, R.I., Christensen, J.L., Weissman, I.L., and Wagers, A.J. (2004b). Determinants of skeletal muscle contributions from circulating cells, bone marrow cells, and hematopoietic stem cells. *Stem Cells* *22*, 1292–1304.
- Stromberg, A., Jansson, M., Fischer, H., Rullman, E., Hagglund, H., and Gustafsson, T. (2013). Bone marrow derived cells in adult skeletal muscle tissue in humans. *Skeletal Muscle* *3*, 12.
- Su, X., Paris, M., Gi, Y.J., Tsai, K.Y., Cho, M.S., Lin, Y.L., Biernaskie, J.A., Sinha, S., Prives, C., Pevny, L.H., et al. (2009). Tap63 prevents premature aging by promoting adult stem cell maintenance. *Cell Stem Cell* *5*, 64–75.
- Valiente-Alandi, I., Albo-Castellanos, C., Herrero, D., Arza, E., Garcia-Gomez, M., Segovia, J.C., Capecchi, M., and Bernad, A. (2015). Cardiac *Bmi1*(+) cells contribute to myocardial renewal in the murine adult heart. *Stem Cell Res. Ther.* *6*, 205.
- Volk, S.W., and Bohling, M.W. (2013). Comparative wound healing—are the small animal veterinarian's clinical patients an improved translational model for human wound healing research? *Wound Repair Regen.* *21*, 372–381.
- Wagers, A.J., Sherwood, R.I., Christensen, J.L., and Weissman, I.L. (2002). Little evidence for developmental plasticity of adult hematopoietic stem cells. *Science* *297*, 2256–2259.
- Wakabayashi, M., Ito, Y., Hamazaki, T.S., and Okochi, H. (2010). Efficient myogenic differentiation of murine dermal Sca-1 (-) cells via initial aggregation culture. *Tissue Eng.* *16*, 3251–3259.
- Wang, X., Ge, J., Tredget, E.E., and Wu, Y. (2013). The mouse excisional wound splinting model, including applications for stem cell transplantation. *Nat. Protoc.* *8*, 302–309.
- Watts, G.T., Grillo, H.C., and Gross, J. (1958). Studies in wound healing: II. The role of granulation tissue in contraction. *Ann. Surg.* *148*, 153–160.
- White, J.D., and Grounds, M.D. (2003). Harnessing the therapeutic potential of myogenic stem cells. *Cytotechnology* *41*, 153–164.
- Wojciechowicz, K., Gledhill, K., Ambler, C.A., Manning, C.B., and Jahoda, C.A. (2013). Development of the mouse dermal adipose layer occurs independently of subcutaneous adipose tissue and is marked by restricted early expression of FABP4. *PLoS One* *8*, e59811.